Thermodynamics of radiation-balanced lasing

Carl E. Mungan

Department of Physics, U.S. Naval Academy, Annapolis, Maryland 21402-5026

Athermal lasers dispose of their waste heat in the form of spontaneous fluorescence (i.e., by laser cooling) to avoid warming the medium. The thermodynamics of this process is discussed both qualitatively and quantitatively from the point of view of the first and second laws. The steady-state optical dynamics of an ytterbium-doped $KGd(WO_4)_2$ fiber is analyzed as a model radiation-balanced solid-state laser. A Carnot efficiency for all-optical amplification is derived in terms of the energy and entropy transported by the pump, fluorescence, and laser beams. This efficiency is compared with the performance of the model system. © 2003 Optical Society of America

OCIS codes: 140.3320, 140.6810, 000.6850.

1. INTRODUCTION

Laser cooling of a variety of condensed materials has been demonstrated experimentally within the past decade: Yb^{3+} doped in heavy metal fluoride glasses[1–3] such as ZBLANP and in the crystals[4,5] KGW and YAG, Tm^{3+} in ZBLANP,[6] ethanol solutions of the organic dyes[7,8] Rhodamine 6G and Rhodamine 101, and GaAs-based semiconductor heterostructures.[9,10] In all these cases the cooling proceeds by pumping between specific sublevels within a pair of electronic bands. These individual sublevels are sufficiently closely spaced (compared to a typical thermal energy of kT) that phonon coupling reduces the pair of bands to a quasi-two-level system. Cooling is achieved by pumping of the material at a wavelength longer than the wavelength λ_F that corresponds to the mean fluorescence photon energy. That is, anti-Stokes fluorescence is responsible for the extraction of thermal energy from the medium.

All these materials also support laser action. This is not surprising because optically pumped lasing is essentially laser cooling run in reverse.[11] For a conventional laser, the Stokes energy shift between the pump photons (of wavelength λ_P corresponding to energy $E_P = hc/\lambda_P$) and the laser output photons (with wavelength λ_L and energy $E_L = hc/\lambda_L$) is commonly called the quantum defect, $E_P - E_L$, and appears as heat in the laser medium. Excess heating can lead to undesirable changes in material parameters (e.g., thermal expansion), to optical aberrations of the beam (defocusing and depolarization), and to fractures or chemical changes in the active material. Such effects limit the performance of high-power lasers, and great effort is expended toward the control of heat (e.g., by circulating coolants, zigzag beam geometry, wavefront corrections, and materials engineering). A novel solution to this problem is to avoid depositing any heat within the laser medium by using an approach known as radiation-balanced or athermal lasing.[12] The basic idea is illustrated in Fig. 1 and consists in optically pumping the system at a wavelength intermediate between the mean fluorescence wavelength and the output lasing wavelength, $\lambda_F < \lambda_P < \lambda_L$, to balance the anti-Stokes

cooling that is due to the spontaneous emission against the Stokes heating from the stimulated emission.

In the present paper the thermodynamics of this self-cooled lasing mechanism is explored. First, a qualitative overview of the admissibility and practicality of such a device from the point of view of the first and second laws of thermodynamics is presented. Next, as a prelude to a more-quantitative analysis, the theory of radiation-balanced lasing is reviewed. Although this theory is in principle already contained in two key references,[4,12] these two sources use different notation and were not specifically applied to a model device. A single-pass edge-pumped fiber amplifier design is considered here. In Section 4 a Carnot efficiency is derived for all-optical amplification from consideration of the radiative transport of energy and entropy.[13] The results are compared with the internal efficiency of an ideal Yb:KGW athermal laser.

2. SIMPLE HEAT-ENGINE PICTURE

In the analysis of a conventional solid-state laser, the role of spontaneous fluorescence is usually assumed to be negligible compared with the stimulated excitation–relaxation cycle driving the dynamics. This is equivalent to ignoring the arrow labeled λ_F in Fig. 1. The resultant energy-level scheme could represent an Yb:YAG laser, for example.[14] The energy difference between an output laser photon and the input pumped transition appears as heat in the host medium, Q_{host}, typically in the form of phonons connecting the pump and laser sublevels. The thermodynamics of the process is compactly characterized by the textbook-style sketch in Fig. 2. Here, the output laser beam is described as work, W_{beam}, in accordance with the Carathéodory viewpoint.[15] That is, ideal laser radiation is able to raise a weight without inducing any other permanent changes in the environment. A mechanism for doing so is Hertzberg's photon engine,[16] wherein the absorbed radiation increases the pressure in a supersonic gaseous beam, thereby driving a turbine with an efficiency that can theoretically equal 100% for an arbitrarily high-fluence, coherent source. From another
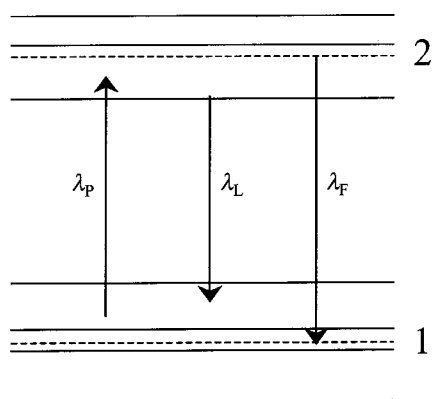
Fig. 1.   Prototypical energy-level scheme for a radiation-balanced laser.   Two bands of energy sublevels are indicated: the ground-state manifold, labeled 1, and the excited-state group, 2.   For example, these bands could represent the $^2F_{7/2}$ and $^2F_{5/2}$ multiplets of Yb^{3+}, the S_0 and S_1 singlet states of an organic dye, or the valence and conduction bands of an intrinsic semiconductor.   The dashed lines represent centroids over the equilibrium population distributions in the two states, under the assumption that each multiplet has ample time to thermalize after any of the indicated optical transitions occurs.   In that case, the mean fluorescence wavelength λ_F is independent of the optical pump and output lasing wavelengths, λ_P and λ_L, respectively.
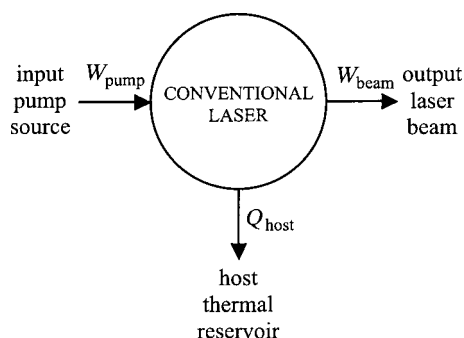

Fig. 2.   Thermodynamic diagram of a conventional laser system. The pump source here is considered to perform work W_{pump} on the laser medium, for example by means of an electrical discharge.   In this and Figs. 3 and 4, input work (W) is labeled at the left, output heat (Q) at the bottom, output work at the right, and input heat at the top of the circled device.

point of view, if the laser beam occupies only a single optical mode, then the entropy that it carries is zero.[17]   By contrast, blackbody radiation (a form of heat transfer) is maximally disordered by virtue of being broadband, unpolarized, and both spatially and temporally incoherent.

In steady state, the first law of thermodynamics requires that the energy input per cycle equal the energy output: $W_{pump} = W_{beam} + Q_{host}$.   This process also satisfies the second law in that some work has been irreversibly converted into waste heat.   It would be a violation of the Kelvin–Planck version of the second law to attempt to design a conventional laser with $\lambda_L < \lambda_P$ by supplying the extra energy thermally.   In other words, a cw laser cooler cannot have a coherent optical output beam.[18] (For example, anti-Stokes Raman laser shifters necessarily have efficiencies far below unity.)

Schematically, an ideal radiation-balanced laser can be thought of as a conventional laser ganged together with an optical refrigerator, as diagrammed in Fig. 3.   The key innovation is the use of the same optical pump source to run both machines, $W_{pump} = W_{pump}^{laser} + W_{pump}^{fridge}$, divided in just such a manner as to ensure that all the heat (Q_{host}) generated by the laser is removed by the refrigerator (fridge).   In keeping with the preceding discussion, the spontaneous fluorescence is labeled heat, $Q_{fluorescence}$, and escapes into the environment.

Although the device sketched in Fig. 3 might be useful as a frequency downconverter, it omits a practical aspect of the physics of athermal lasing.   Because $W_{beam} = W_{pump} - Q_{fluorescence}$, the laser output is necessarily less energetic than the input.   An intended application is a compact high-power laser, so presumably a single, high-quality laser source is not already available as a driver. The implication is that the pump should not be represented as work alone, i.e., as "high-grade" optical energy that transfers no entropy, to use the nomenclature of Landsberg and Tonge.[19]

However, it is impossible for the pump to be an optical source of pure heat, such as blackbody radiation from a thermal flash lamp.   The Clausius statement of the second law of thermodynamics requires that the refrigerator be pumped by work, W_{pump}^{fridge}, and not by heat.   Furthermore, laser pumping is typically more efficient than broadband flash-lamp pumping, owing to a better overlap between the source emission and the laser absorption. One concludes that the pump energy should be delivered partly in the form of work and partly in the form of heat, $E_P = W_{pump} + Q_{pump}$, as sketched in Fig. 4.   In practice, the source would probably consist of a set of mutually incoherent diode lasers.[20]   One might thus view a radiation-balanced system as a coherent beam combiner, in which the improvement in beam quality of the output laser compared with the set of input lasers is at minimum compensated for by the entropy carried away by the fluorescence signal.   Just as for a conventional laser, it is therefore clear that the efficiency must drop to zero as the Stokes shift, $\lambda_L - \lambda_P$, and hence the fluorescence energy, $E_F = Q_{fluorescence}$, is made to vanish.
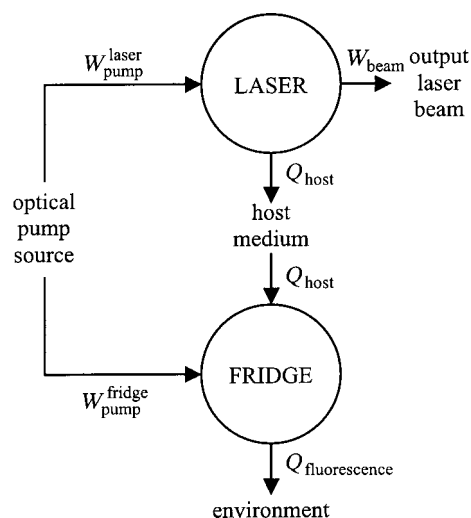

Fig. 3.   Cartoon of an idealized athermal laser pumped by an optical source of work.   No net heat is deposited in the host; the spontaneously emitted radiation is assumed eventually to escape the medium and get dumped onto some externally shielded absorber.
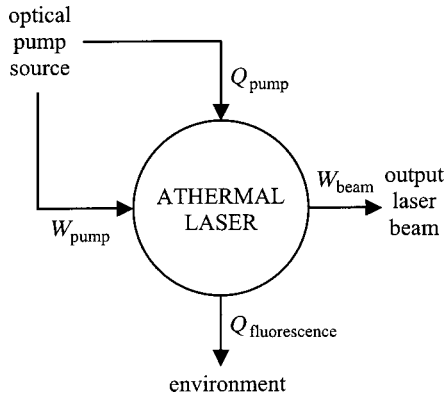
Fig. 4.   Energy-flow diagram for a practical radiation-balanced laser.   To make contact with the subsequent quantitative analysis, note that the output laser energy is $E_L = W_{\text{beam}}$ per cycle.

To review, the cartoon in Fig. 3 properly depicts the energy flows in the system and can be used to calculate the so-called thermodynamic first-law efficiency[19] (the ratio of the output laser power to the input pump power).   However, the second law of thermodynamics further restricts the performance of the system by considering not merely the energies but how much is useful or available for conversion into high-grade form.   Specifically, a computation of the free energy requires knowledge of the radiation entropy.   The product of the entropy and the thermodynamic brightness temperature[19] can be defined as the heat transported by the pump beam, as sketched in Fig. 4.

3.   OPTICAL ANALYSIS OF RADIATION-BALANCED LASING

Assume that the optical system depicted in Fig. 1 satisfies the three basic conditions for laser cooling: rapid intraband thermalization within each manifold (i.e., level splittings small compared to kT); purely radiative interband relaxation (i.e., a bandgap large compared to the energies of the phonons and local modes); and the absence of competitive excited-state absorption, energy transfer, and absorption by nonradiative background impurities.   In that case, the excited-to-ground-state spontaneous emission has a characteristic mean photon energy $E_F = h\nu_F = hc/\lambda_F$, which can be computed from the measured fluorescence intensity $I_{\nu F}\mathrm{d}\nu = I_{\lambda F}\mathrm{d}\lambda$ (W/cm^2).   For this purpose, the spectral intensity must be converted to photon spectral flux density, $I_{\nu F}/h\nu$ (s^{-1} cm^{-2} Hz^{-1}).   That is, the averaging of photon energy E must be weighted by the spontaneous emission rate rather than by power:

$$E_F = \frac{\int EI_{\nu F}h^{-1}\nu^{-1}\mathrm{d}\nu}{\int I_{\nu F}h^{-1}\nu^{-1}\mathrm{d}\nu} \Rightarrow \lambda_F = \frac{\int \lambda I_{\lambda F}\mathrm{d}\lambda}{\int I_{\lambda F}\mathrm{d}\lambda}. \quad (1)$$

The second form is useful for typical spectrometric data measured in fixed-slit wavelength increments.   In the case of a biaxial sample, relation (1) must be generalized by separate summing of the numerators and the denominators over the intensities emitted along the three crystallographic axes.[21]   For Yb:KGW this gives $\lambda_F = 993$ nm.

Two conditions are necessary for radiation balance. First, the absorption rate density (cm^{-3} s^{-1}) must equal the sum of the stimulated and spontaneous emission rate densities:

$$\frac{I_P}{h\nu_P}(N_1\sigma_{\text{AP}} - N_2\sigma_{\text{EP}}) = \frac{I_L}{h\nu_L}(N_2\sigma_{\text{EL}} - N_1\sigma_{\text{AL}}) + \frac{N_2}{\tau}. \quad (2)$$

Throughout this paper, subscript P denotes the optical pump; L, the output laser beam; and F, the spontaneous fluorescence.   The optical intensities and frequencies are denoted I and ν, respectively.   The volume densities (cm^{-3}) of active ions in the ground and excited states are labeled N_1 and N_2.   In accordance with the discussion beginning this section, it is assumed that $N_1 + N_2 = N$ is the constant total density.   For a doped solid, this density can be calculated from atomic fractional concentration n as $nN_A\rho/M$, where M is the molecular weight when one substituent atom per formula unit is assumed, ρ is the mass density of the pure host, and N_A is Avogadro's number.   Lifetime τ can be determined by time-resolved fluorescence.   Finally, σ_{AP} and σ_{AL} are the absorption cross sections at the pump and the output laser wavelengths, respectively, and σ_{EP} and σ_{EL} are the corresponding emission cross sections.   (Note that the absorption and emission cross sections are not in general equal to each other at the same wavelength, because they are sums over a large number of overlapping ground-state-sublevel to excited-state-sublevel transitions.   To emphasize this fact, they are sometimes called the effective cross sections.)   The absorption cross section is simply the unsaturated absorption coefficient (cm^{-1}) divided by N.   In contrast, the emission cross section must be determined either from the fluorescence spectrum by use of the Füchtbauer–Ladenburg equation or from the absorption cross section by the principle of reciprocity.[22]   The six independent polarized absorption and emission cross sections for Yb:KGW have been graphed and discussed in Ref. 21.

The second condition for athermal lasing is that the absorbed and emitted power densities (W/cm^3) must balance:

$$I_P(N_1\sigma_{\text{AP}} - N_2\sigma_{\text{EP}}) = I_L(N_2\sigma_{\text{EL}} - N_1\sigma_{\text{AL}}) + \frac{N_2h\nu_F}{\tau}. \quad (3)$$

It has been implicitly assumed in writing Eqs. (2) and (3) that the pump and output laser bandwidths are narrower than the linewidths of the interband transitions.   (Otherwise it would be necessary to integrate the spectral intensities over the wavelength-dependent cross sections.)   Substitute $N_1 = N - N_2$ into these equations to eliminate the unknown N_1, where N, τ, and ν_F are fixed for a particular material at a given operating temperature.   Next, the performance of the system is optimized by choice of ν_P and ν_L according to the procedure discussed in Ref. 4; this consequently determines the values of the four optical pump and output laser cross sections.   Equations (2) and (3) can then be solved simultaneously for I_L and N_2 in terms of pump intensity I_P.   This sets the initial conditions at the input face of an athermal amplifier.

However, the lasing intensity must subsequently grow as it propagates through the crystal (in a direction defined to be z) according to the gain equation

$$\frac{dI_L}{dz} = I_L(N_2\sigma_{EL} - N_1\sigma_{AL}).\tag{4}$$

Consequently $I_P(z)$ is not arbitrary for $z > 0$.

Eliminating the population densities N_1 and N_2 from Eq. (4) by use of Eqs. (2) and (3) [cf. Eq. (7) below] and integrating lead to

$$\frac{I_L(z)}{I_L(0)} = \frac{I_{L_{min}}}{I_L(0)}\frac{\beta_P - \beta_L}{\beta_P}\left\{\ln\left[\frac{I_L(z)}{I_L(0)}\right] + N\sigma_{AL}z\right\} + 1.\tag{5}$$

Equation (5) can be solved for $I_L(z)$ by iteration in a spreadsheet. It is therefore convenient to express $I_P(z)$ and $N_2(z)$ in terms of $I_L(z)$. After some algebra, Eqs. (2) and (3) can be rearranged as

$$\frac{I_{P_{min}}}{I_P} = 1 - \frac{I_{L_{min}}}{I_L},\tag{6}$$

$$\frac{N}{N_2} = \frac{1}{\beta_L} + \left(\frac{1}{\beta_P} - \frac{1}{\beta_L}\right)\frac{I_{L_{min}}}{I_L}.\tag{7}$$

Equations (5)–(7) have been written in terms of the two quantities

$$I_{P_{min}} = \frac{\beta_P\beta_L}{\beta_P - \beta_L}\frac{h\nu_P}{\sigma_{AP}\tau}\frac{\nu_F - \nu_L}{\nu_P - \nu_L},$$

$$I_{L_{min}} = \frac{\beta_P\beta_L}{\beta_P - \beta_L}\frac{h\nu_L}{\sigma_{AL}\tau}\frac{\nu_F - \nu_P}{\nu_P - \nu_L},\tag{8}$$

where $\beta_P \equiv \sigma_{AP}/(\sigma_{AP} + \sigma_{EP})$ and $\beta_L \equiv \sigma_{AL}/(\sigma_{AL} + \sigma_{EL})$. As explained in Ref. 12, these quantities represent the minimum pump and laser intensities required for sustaining radiation balancing. In other words, I_L is infinite when $I_P = I_{P_{min}}$, and I_L decreases monotonically to $I_{L_{min}}$ as $I_P \to \infty$. This completes the solution.

Now apply the solution to the following model system: Ytterbium-doped KGW, specifically KGd(WO$_4$)$_2$ with 3.5% of the gadolinium ions replaced by Yb^{3+}, has the highest figures of merit for radiation-balanced lasing of any evaluated material.[4] Its performance is optimized by pumping with a polarization at a wavelength of λ_P = 1001 nm and amplifying a b-polarized laser beam that has a wavelength of λ_L = 1042 nm. The corresponding cross sections are σ_{AP} = 1.53 pm^2, σ_{EP} = 5.11 pm^2, σ_{AL} = 0.083 pm^2, and σ_{EL} = 1.88 pm^2. To keep the thermo-optical calculations simple, consider the single-pass edge-pumped amplifier design sketched in Fig. 5. The laser crystal is in the shape of an 11-cm-long fiber with a 1 mm × 1 mm square cross section. Its length has been chosen to equal 2/($N\sigma_{AL}$), where N = 2.2 × 10^{20}/cm^3, in accordance with the suggestion of Ref. 12. The transverse dimensions of the slab are small, so the pump intensity remains approximately constant across its width.[23] (It is assumed that the sides of the slab are antireflection coated at the pump wavelength and the end faces at the output laser wavelength.) Otherwise the
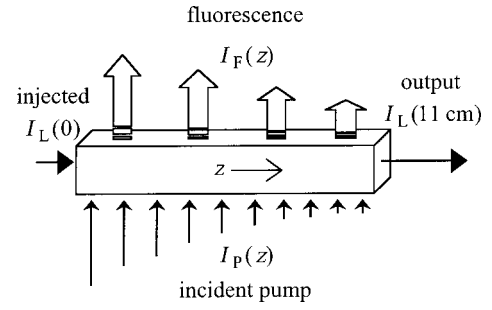

Fig. 5. Single-pass edge-pumped athermal amplifier in the shape of a 1 mm × 1 mm × 110 mm fiber of KGW + 3.5 at. % Yb^{3+}. A set of 110 pump beams is distributed uniformly along its bottom face. The amplified beam and each pump beam have 1 mm × 1 mm top-hat spatial profiles. For clarity the fluorescence is shown escaping from the top side of the slab only.

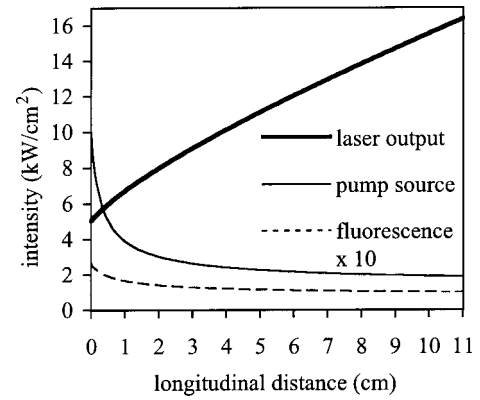Fig. 6. I_L, I_P, and I_F versus z for the laser amplifier sketched in Fig. 5. The fluorescence intensity (expanded vertically by a factor of 10) is that which crosses the surface of the fiber and is taken to be hemispherically isotropic; the spectral shift that is due to photon recycling by repeated absorption and reemission is neglected.

longitudinally propagating laser beam could not be a plane wave but would have to have a specially tailored spatial profile. The KGW crystal can be conceptually divided into 110 cubic segments, each with a volume of δV = l^3, where l = 1 mm is the step size used in numerically evaluating Eq. (5) for $I_L(z)$ from injection to output. A separate pump source excites each of these volume elements.[24] The brightest pump is needed at the injection end. Again following the recommendations of Ref. 12, it will be assumed to have an intensity of $I_P(0)$ = 10 kW/cm^2 and thus 100 W of power.[25] Given that τ = 600 μs for Yb^{3+}-doped KGW, the minimum intensities in Eq. (8) are determined to be $I_{P_{min}}$ = 1.37 kW/cm^2 and $I_{L_{min}}$ = 4.36 kW/cm^2. Thus $I_P(0)$ is comfortably larger than $I_{P_{min}}$, as required for efficient operation.

The injection intensity of the amplified laser beam is calculated from Eq. (6) to be $I_L(0)$ = 5.05 kW/cm^2, which is about as close in value to $I_{L_{min}}$ as one might realistically hope to achieve. The growth in strength of this laser beam as it propagates along the slab is now solved by stepping along of Eq. (5) in increments of δz = 1 mm. The result is graphed as the thick curve in Fig. 6, which quickly settles into a nearly linear slope.[12] The required pump intensity I_P to sustain this amplification is plotted

as the thin continuous curve, calculated from Eq. (6). Were the fiber to be semi-infinite in length, then I_P would asymptotically approach $I_{P_{\min}}$ as $z \to \infty$.

The efficiency calculations also require knowledge of the external fluorescence intensity at the surface of the crystal. Recalling that its power density is given by the last term in Eq. (3), one can compute this intensity as

$$I_F = \frac{h\,\nu_F N_2}{\tau}\,\frac{\delta V}{\delta A_s} = \frac{h\,\nu_F N_2 l}{4\,\tau}, \tag{9}$$

where $\delta V = l^3$ is the volume of each pumped element, with an external surface area of $\delta A_s = 4l^2$. Note that fluorescence generated in element i (where i varies from 1 to 110 along the length of the fiber in Fig. 5) and emitted rightward into the adjacent element $i + 1$ is approximately balanced by the spontaneous radiation propagating leftward from emitter $i + 1$ back into i. Hence there is minimal net flux across the end caps of each volume element. (The areas of the entrance and exit faces of the fiber can be neglected.) Equation (9), with Eq. (7) used for calculating N_2, is plotted as the dashed curve in Fig. 6. As the fluorescence energy has merely to balance the quantum defect of the quasi-two-level laser cycle, I_F is small and has consequently been expanded vertically in this figure by a factor of 10.

The analysis in this section was predicated on several idealizations. In particular, radiation trapping of the fluorescence and heating by nonradiative decay processes were neglected. Consider the effect of each of these in turn. The refractive index of KGW is approximately 2.0 for all three crystallographic axes. Suppose that the laser rod is cut such that a is parallel to longitudinal axis z, while b and c span the edges of the 1 mm × 1 mm end faces. (The slight distortion of KGW from tetragonal symmetry has been neglected because the monoclinic angle is only 4° off normal.) The internal fractions of the spontaneously emitted light that have each polarization (i.e., 59% a, 29% b, and 12% c) can be computed from the emission cross sections. These photons are emitted with a dipolar angular distribution and either escape or reflect when they strike a crystal boundary. Light incident at greater than the critical angle of 30° will be trapped; that incident at lower angles can be assumed to escape (in view of the antireflection surface coatings and the internal Brewster angle). Consequently one might expect that a substantial fraction of the fluorescence would be waveguided along the slab. However, those photons will be reabsorbed after traveling only 7 mm on average, thus attenuating the blue end of the fluorescence, where there is a strong overlap between the absorption and the emission cross sections. The net effect of single-photon recycling after integration over solid angles and performance of an absorptance-weighted average over polarizations is to redshift λ_F by 7 nm.

Next consider the effects of nonradiative relaxation. Excited ytterbium ions can transfer their energy to quenching centers or modes, such as foreign rare-earth atoms or host vibrations. This has the effect of shifting λ_F to $\lambda_F^* \equiv \lambda_F/\eta_F$, where the radiative quantum efficiency[21] of Yb:KGW is $\eta_F = 0.987$, resulting in a 13-nm redshift. (Direct absorption of the pump by back-

ground impurities such as transition metals, with absorption coefficient α_b, can also occur in principle,[11] but the tungstate samples do not show convincing evidence that they have done so.[4,21] Modeling its effects would require more-detailed knowledge of its polarization and wavelength dependence.)

The upshot of these two effects is to increase the effective mean fluorescence wavelength, although the exact shift depends on the details of the sample geometry and purity. To compensate for it, the pump wavelength can be detuned to the red. Increasing λ_P from, say, 1001 to 1019 nm decreases σ_{AP} from 1.53 to 0.45 pm². This lowers but does not negate the cooling efficiency,[21] so athermal operation is still possible. More realistically, the initial experimental goal is to reduce rather than eliminate the need for an external coolant.[26]

4. THERMODYNAMIC EFFICIENCY OF THE MODEL SYSTEM

To quantify the thermodynamics of the energy conversion processes within a radiation-balanced laser it is necessary to consider the rates at which both energy (E) and entropy (S) flow through the device.[19] Therefore Fig. 4 is redrawn in the form of Fig. 7. Here $\dot{E}_P$ and $\dot{S}_P$ are the rates at which the active material absorbs energy and entropy from the pump lasers, $\dot{E}_L$ and $\dot{S}_L$ are the net rates with which energy and entropy are added to the amplified laser field, and $\dot{E}_F$ and $\dot{S}_F$ are the rates at which energy and entropy are carried away by spontaneous fluorescence. Assuming steady-state operation, the first law of thermodynamics implies that

$$\dot{E}_P = \dot{E}_L + \dot{E}_F, \tag{10}$$

whereas the second law gives rise to the inequality

$$\dot{S}_L + \dot{S}_F - \dot{S}_P \geq 0. \tag{11}$$

Irreversible processes cause the left-hand side to be strictly greater than zero; examples of such processes are discussed in Ref. 11. (The arrows in Fig. 3 cannot be
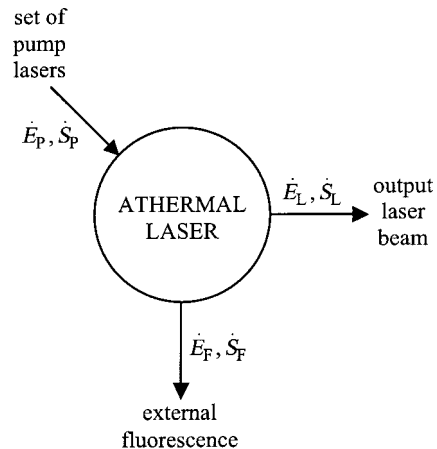

Fig. 7. Energy and entropy transported optically into and out of an athermal laser. The dots denote time derivatives; i.e., $\dot{E}$ is power in units of watts, whereas $\dot{S}$ has units of watts per kelvin, both sometimes referred to as fluxes.

wholly reversed and hence the Carnot efficiency derived below can never be fully attained by an athermal laser.[27])

Introducing the flux temperatures $T_P \equiv \dot{E}_P/\dot{S}_P$, $T_L \equiv \dot{E}_L/\dot{S}_L$, and $T_F \equiv \dot{E}_F/\dot{S}_F$, one can combine Eqs. (10) and (11) to derive an upper limit on the efficiency of optical amplification:

$$\eta \equiv \frac{\dot{E}_L}{\dot{E}_P} \le \frac{1 - T_F/T_P}{1 - T_F/T_L} \approx 1 - T_F\left(\frac{1}{T_P} - \frac{1}{T_L}\right). \quad (12)$$

The last step follows from the fact that the fluorescence carries much lower energy and much higher entropy than both the pumped and the amplified laser beams. It can be written in the Carnot form $(T_h - T_c)/T_h$, where the effective temperatures of the hot and cold reservoirs are $T_h = (1/T_P - 1/T_L)^{-1}$ and $T_c = T_F$, respectively. In the case of an ideal laser output beam (i.e., a beam that occupies a single optical mode), $T_L \to \infty$ and consequently the ideal Carnot efficiency is $\eta_c = 1 - T_F/T_P$.

The optical flux temperatures can be calculated from the flux densities (i.e., energy or entropy per unit time per unit area) of the corresponding beams.[19,28] Specifically, the external fluorescence power is

$$\dot{E}_F = \int I_F \mathrm{d}A_s = 4\int I_F \mathrm{d}A. \quad (13)$$

The first integral is over the surface area A_s of the entire sample. But the fluorescence can be approximated as being symmetrically emitted by the four rectangular faces, each of area $A = 110$ mm^2, in Fig. 5. (For consistency, dA has the same range of integration in every equation in this section.)

The contribution of photons from the ambient surroundings to the entropy flux density is negligible because T_F turns out to be much larger than room temperature. Therefore the rate at which the fluorescence carries off entropy is

$$\dot{S}_F = 4kc \int\int\int [(1 + n_F)\ln(1 + n_F)$$
$$- n_F \ln n_F]\gamma \mathrm{d}E \cos\theta \mathrm{d}\Omega \mathrm{d}A$$
$$= 8\pi kc \int\int [(1 + n_F)\ln(1 + n_F)$$
$$- n_F \ln n_F]\lambda^{-4}\mathrm{d}\lambda \mathrm{d}A, \quad (14)$$

where $\gamma = 2E^2(hc)^{-3}$ is the density of photon states [J^{-1} cm^{-3} sr^{-1}, with the factor of 2 arising from the two independent transverse polarizations (Ref. 17)] and where $\cos\theta$ is the radiometric projection factor. The angular integral gave rise to the factor of π, because the fluorescence is assumed to be isotropically emitted into the outgoing hemisphere about each point on the surface of the crystal. Here n_F is the (dimensionless) fluorescence photon occupation number. It is related to the spontaneous emission spectrum as follows:

$$I_{\lambda F}\mathrm{d}\lambda = \left(c\int En_F\gamma\cos\theta \mathrm{d}\Omega\right)\mathrm{d}E = 2\pi hc^2 n_F\lambda^{-5}\mathrm{d}\lambda$$

$$\Rightarrow n_F = \frac{I_F\lambda^5}{2\pi hc^2}\frac{I_{\lambda F_n}}{\int I_{\lambda F_n}\mathrm{d}\lambda}, \quad (15)$$

where the subscript n on the spectral intensity denotes that the spectrum has been normalized to unity at a peak wavelength $\lambda_{\max}$. (Sometimes $I_{\lambda F_n}$ is called the normalized emission spectral density.)

The power absorbed from the pump sources is

$$\dot{E}_P = \int I_P(N_1\sigma_{\mathrm{AP}} - N_2\sigma_{\mathrm{EP}})l\mathrm{d}A, \quad (16)$$

where the area integral spans the 110 pump beams irradiating the bottom face of the fiber in Fig. 5 and where the absorption has been computed in the linear limit.[23] The rate at which entropy is deposited in the sample is

$$\dot{S}_P = 4\pi kc \int\int [(1 + n_{P_{\mathrm{in}}})\ln(1 + n_{P_{\mathrm{in}}})$$
$$- n_{P_{\mathrm{in}}}\ln n_{P_{\mathrm{in}}}]\lambda^{-4}\mathrm{d}\lambda\mathrm{d}A - 4\pi kc \int\int [(1$$
$$+ n_{P_{\mathrm{out}}})\ln(1 + n_{P_{\mathrm{out}}}) - n_{P_{\mathrm{out}}}\ln n_{P_{\mathrm{out}}}]\lambda^{-4}\mathrm{d}\lambda\mathrm{d}A. \quad (17)$$

Because the pump beams have a top-hat profile directed normal to the sample surface, the projection factor is 1 in this case and hence the angular integration gave 2π rather than π. In analogy with relation (15), the occupation number for pump photons entering the bottom face of the sample is

$$n_{P_{\mathrm{in}}} = \begin{cases} \dfrac{I_P\lambda^5}{4\pi hc^2\Delta\lambda_P} & \lambda \in \Delta\lambda_P \\ 0 & \text{otherwise} \end{cases}, \quad (18)$$

where the spectral profile of each pump source has been approximated as a square pulse with a (small) bandwidth of $\Delta\lambda_P$. Not all the pump photons are absorbed by the sample, and hence their occupation number on exiting the top face of the slab is

$$n_{P_{\mathrm{out}}} = n_{P_{\mathrm{in}}}(1 - N_1\sigma_{\mathrm{AP}}l + N_2\sigma_{\mathrm{EP}}l). \quad (19)$$

The area integrals over dA in Eqs. (13)–(17) can be replaced by l^2 times a summation over the 110 elements that compose the fiber. Approximating[25] λ by λ_P and dλ by $\Delta\lambda_P = 4$ nm in Eq. (17) then results in

$$T_P = \frac{\lambda_P^4 l \sum I_P(z_i)\alpha_i}{4\pi kc\Delta\lambda_P \sum s_{Pi}}. \quad (20)$$

Whereas it is not hard to integrate Eq. (14) exactly over the sum of the three polarized emission spectra graphed in Ref. 21, the dominant a-polarized spectrum is sufficiently narrow that an expression similar to Eq. (18) suffices to approximate n_F, and consequently the analog of Eq. (20) becomes

$$T_F = \frac{\lambda_{\max}^4 \sum I_F(z_i)}{2\pi kc\Delta\lambda_F \sum s_{Fi}}. \qquad (21)$$

The averaged fluorescence spectrum for Yb:KGW is found to peak at $\lambda_{\max} = 982$ nm with a bandwidth of $\Delta\lambda_F = \int I_{\lambda F_n} d\lambda = 28$ nm. The summations in Eqs. (20) and (21) run over i from 1 to 110, and the new variables introduced in these expressions are

$$\alpha_i = N_1(z_i)\sigma_{AP} - N_2(z_i)\sigma_{EP},$$

$$s_{Fi} = (1 + n_{Fi})\ln(1 + n_{Fi}) - n_{Fi}\ln n_{Fi},$$

$$s_{Pi} = (1 + n_{P i_{\text{in}}})\ln(1 + n_{P i_{\text{in}}}) - n_{P i_{\text{in}}}\ln n_{P i_{\text{in}}}$$
$$- (1 + n_{P i_{\text{out}}})\ln(1 + n_{P i_{\text{out}}}) + n_{P i_{\text{out}}}\ln n_{P i_{\text{out}}},$$

$$n_{P i_{\text{in}}} = \frac{I_P(z_i)\lambda_P^5}{4\pi hc^2\Delta\lambda_P}, \qquad n_{P i_{\text{out}}} = n_{P i_{\text{in}}}(1 - \alpha_i l),$$

$$n_{Fi} = \frac{I_F(z_i)\lambda_{\max}^5}{2\pi hc^2\Delta\lambda_F}.$$

Using the data graphed in Fig. 6, one finds that $n_{P_{\text{in}}}$ decreases from 34 at $z = 0$ to 6 at $z = 11$ cm. These values are large owing to the high brightness of the pump sources. Over the same range, n_F drops from 0.23 to 0.088.

Finally, the flux temperatures are computed from Eqs. (20) and (21) to be $T_P = 11,000$ K and $T_F = 4500$ K, implying that the Carnot efficiency for this model athermal amplifier is $\eta_c = 60\%$. In comparison, its internal optical efficiency is

$$\eta_o = \frac{I_L(11 \text{ cm}) - I_L(0)}{\sum I_P(z_i)\alpha_i l} = 17\%, \qquad (22)$$

assuming 100% radiative quantum efficiency. This agrees with the value tabulated in Ref. 4, thereby confirming the calculations.

5. CONCLUSION

Because an Yb:KGW athermal laser has an optical efficiency of 17%, the gain for the model system depicted in Fig. 5 is $G \equiv I_L(11 \text{ cm})/I_L(0) = 3.2$ for an absorbed pump power of $\sum I_P(z_i)\alpha_i l^3 = 660$ W. The maximum possible gain that could be achieved with *any* kind of optical device (with the same injected laser and absorbed pump powers and bandwidths) is 8.9, which would require a fully reversible photon amplifier that had an efficiency of 60%. This difference between η_o and η_c reflects the generation of entropy S_g by processes that are internal to the athermal amplifier. In contrast, the Carnot efficiency considers only the optical beams that cross a control surface surrounding the device.[29] But, seen from another point of view, 17% is a constant for an Yb:KGW radiation-balanced laser (given wavelengths λ_F, λ_P, and λ_L) *regardless* of its geometry and the nature of its optical sources. That is, the ratio of the stimulated emission and absorption power densities is

$$\eta_o \equiv \frac{I_L(N_2\sigma_{EL} - N_1\sigma_{AL})}{I_P(N_1\sigma_{AP} - N_2\sigma_{EP})} = \frac{\lambda_P - \lambda_F}{\lambda_L - \lambda_F} \qquad (23)$$

from Eqs. (2) and (3). In contrast, the 60% result depends on, for example, the bandwidth of the pump lasers.

In particular, the highest Carnot efficiencies result only when the system is pumped into saturation, as can be seen from Fig. 8, where $I_P(0)$ has been varied but all other user-defined parameters have been kept the same. The left-hand edge of the figure corresponds to pumping at the minimum intensity, $I_{P_{\min}}$, and the right-hand edge is close to the intensity at which the model system described in this paper was driven. The dashed line across the middle of the figure indicates the intensity at which $I_P(0) = I_{P_{\text{sat}}}$. This is the pump saturation intensity defined in Ref. 12, which explains the knee in the curve. However, a linear graph results if η_c is plotted against *absorbed* rather than incident pump power.

It is helpful to review the origin of the numerical value of η_c. The amplified laser beam was assumed to transport no entropy (i.e., $T_L \to \infty$). Therefore the spontaneous emission field must carry away all the entropy absorbed from the pump. For a given pump power, wavelength, and bandwidth, this fact determines the minimum required fluorescence power and hence the maximum possible thermodynamic efficiency.[30]

The increase in the Carnot efficiency with pump absorption in Fig. 8 can now be understood conceptually as follows: The energy of a collection of photons of fixed mean frequency and angular divergence scales linearly with the number of photons. In contrast, the entropy of the set depends not only on the number but also on the energy distribution of the photons. If all the photons are in the same quantum state, the beam has zero entropy. (This again is what is meant by categorizing ideal laser radiation as "pure work.") However, if the photons are spread into a blackbody spectrum, the beam transports heat with an entropy that corresponds to the actual brightness temperature of the spectrum.[31] It is therefore
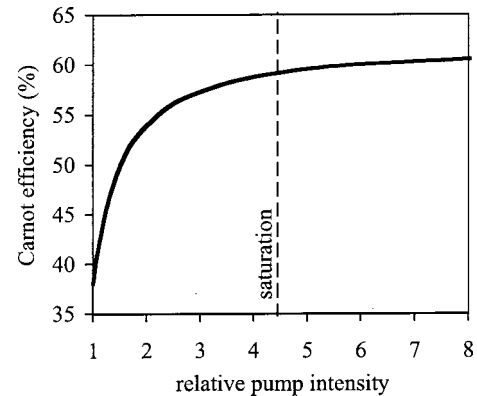

Fig. 8. Carnot efficiency η_c for the athermal amplifier sketched in Fig. 5 as a function of $I_P(0)/I_{P_{\min}}$. When the system is pumped at its minimum operational intensity, 410 W of pump power is absorbed and $\eta_c = 38\%$. The pump intensity saturates when $I_{P_{\text{sat}}}/I_{P_{\min}} = (\beta_P - \beta_L)/\beta_L = 4.45$; at this point, it requires 640 W of pump power to run the Yb:KGW laser and $\eta_c = 59\%$. In the limit as $I_P(0) \to \infty$, the system absorbs only another 50 W of power, and its Carnot efficiency barely increases to 62%.

clear that, as photons are added to the pump beam, the entropy that the beam carries *per photon* decreases because it is becoming more sharply peaked. This is also true for the fluorescence, except that, as I_F is increased, the entropy that it transports per photon does not decrease as rapidly as does the pump beam. There are three reasons for this: The spontaneously emitted light is less intense, broader in bandwidth, and distributed over a larger range of solid angles than is the pump radiation. [These are the relevant factors that appear in Eqs. (20) and (21).] Therefore, because the entropy absorbed by the pump balances the entropy carried away by the fluorescence, the number of fluorescence photons grows sublinearly with the number of absorbed pump photons. This leaves more of the pump photons for conversion into laser photons, thus improving the Carnot efficiency.

ACKNOWLEDGMENTS

REFERENCES AND NOTES

1. R. I. Epstein, M. I. Buchwald, B. C. Edwards, T. R. Gosnell, and C. E. Mungan, "Observation of laser-induced fluorescent cooling of a solid," Nature **377**, 500–503 (1995).
2. J. Fernández, A. Mendioriz, A. J. García, R. Balda, and J. L. Adam, "Anti-Stokes laser-induced internal cooling of Yb^{3+}-doped glasses," Phys. Rev. B **62**, 3213–3217 (2000).
3. A. Rayner, M. E. J. Friese, A. G. Truscott, N. R. Heckenberg, and H. Rubinsztein-Dunlop, "Laser cooling of a solid from ambient temperature," J. Mod. Opt. **48**, 103–114 (2001).
4. S. R. Bowman and C. E. Mungan, "New materials for optical cooling," Appl. Phys. B **71**, 807–811 (2000).
5. R. I. Epstein, J. J. Brown, B. C. Edwards, and A. Gibbs, "Measurements of optical refrigeration in ytterbium-doped crystals," J. Appl. Phys. **90**, 4815–4819 (2001).
6. C. W. Hoyt, M. Sheik-Bahae, R. I. Epstein, B. C. Edwards, and J. E. Anderson, "Observation of anti-Stokes fluorescence cooling in thulium-doped glass," Phys. Rev. Lett. **85**, 3600–3603 (2000).
7. C. Zander and K. H. Drexhage, "Cooling of a dye solution by anti-Stokes fluorescence," in *Advances in Photochemistry*, D. C. Neckers, D. H. Volman, and G. von Bünau, eds. (Wiley, New York, 1995), Vol. 20, pp. 59–78.
8. J. L. Clark and G. Rumbles, "Laser cooling in the condensed phase by frequency up-conversion," Phys. Rev. Lett. **76**, 2037–2040 (1996).
9. H. Gauck, T. H. Gfroerer, M. J. Renn, E. A. Cornell, and K. A. Bertness, "External radiative quantum efficiency of 96% from a GaAs/GaInP heterostructure," Appl. Phys. A **64**, 143–147 (1997).
10. E. Finkeissen, M. Potemski, P. Wyder, L. Viña, and G. Weimann, "Cooling of a semiconductor by luminescence up-conversion," Appl. Phys. Lett. **75**, 1258–1260 (1999).
11. C. E. Mungan and T. R. Gosnell, "Laser cooling of solids," in *Advances in Atomic, Molecular, and Optical Physics*, B. Be-
    derson and H. Walther, eds. (Academic, San Diego, Calif., 1999), Vol. 40, pp. 161–228.
12. S. R. Bowman, "Lasers without internal heat generation," IEEE J. Quantum Electron. **35**, 115–122 (1999).
13. M. A. Weinstein, "Thermodynamic limitation on the conversion of heat into light," J. Opt. Soc. Am. **50**, 597–602 (1960).
14. H. W. Bruesselbach, D. S. Sumida, R. A. Reeder, and R. W. Byren, "Low-heat high-power scaling using InGaAs-diode-pumped Yb:YAG lasers," IEEE J. Sel. Top. Quantum Electron. **3**, 105–116 (1997).
15. G. Laufer, "Work and heat in the light of (thermal and laser) light," Am. J. Phys. **51**, 42–43 (1983).
16. W. H. Christiansen and A. Hertzberg, "Gasdynamic lasers and photon machines," Proc. IEEE **61**, 1060–1072 (1973).
17. L. Landau, "On the thermodynamics of photoluminescence," J. Phys. (Moscow) **10**, 503–506 (1946).
18. O. Kafri and R. D. Levine, "Thermodynamics of adiabatic laser processes: optical heaters and refrigerators," Opt. Commun. **12**, 118–122 (1974).
19. P. T. Landsberg and G. Tonge, "Thermodynamic energy conversion efficiencies," J. Appl. Phys. **51**, R1–R20 (1980).
20. Th. Graf, J. E. Balmer, and H. P. Weber, "Entropy balance of optically pumped cw lasers," Opt. Commun. **148**, 256–260 (1998).
21. C. E. Mungan, S. R. Bowman, and T. R. Gosnell, "Solid-state laser cooling of ytterbium-doped tungstate crystals," in *Lasers 2000*, V. J. Corcoran and T. A. Corcoran, eds. (STS, McLean, Va., 2001), pp. 819–826.
22. L. D. DeLoach, S. A. Payne, L. L. Chase, L. K. Smith, W. L. Kway, and W. P. Krupke, "Evaluation of absorption and emission properties of Yb^{3+} doped crystals for laser applications," IEEE J. Quantum Electron. **29**, 1179–1191 (1993).
23. An upper limit on the pump absorption is $N\sigma_{AP}l = 34\%$, where $l = 1$ mm.
24. Each pump source need not be a separate laser: The unabsorbed pump radiation can be recycled from one volume element to another.
25. The pump lasers are assumed to have a bandwidth of $\Delta\lambda_P = 4$ nm. This value is typical for commercially available 100-W cw solid-state lasers at ~1-μm wavelength.
26. In S. R. Bowman, N. W. Jenkins, S. P. O'Connor, and B. J. Feldman, "Sensitivity and stability of a radiation-balanced laser system," IEEE J. Quantum Electron. **38**, 1339–1348 (2002), radiation-balanced lasing is calculated to be stable against perturbations in the intensities and wavelengths of the optical pump and amplified laser beams. The operating temperature of the tungstate crystal will change to reestablish balance. In addition, compared with the values used in the present paper, a slightly higher value of the radiative quantum efficiency ($\eta_F = 0.990$) and a lower value of the excited-state lifetime ($\tau = 334$ μs) are measured for an Yb:KGW sample that is thin enough to avoid fluorescence reabsorption.
27. R. Kosloff and E. Geva, "Quantum refrigerators in quest of the absolute zero," J. Appl. Phys. **87**, 8093–8097 (2000).
28. B. C. Edwards, M. I. Buchwald, and R. I. Epstein, "Development of the Los Alamos solid-state optical refrigerator," Rev. Sci. Instrum. **69**, 2050–2055 (1998).
29. Yu. T. Mazurenko, "A thermodynamic treatment of the process of photoluminescence," Opt. Spectrosc. (USSR) **18**, 24–26 (1965).
30. Yu. P. Chukova, "The region of thermodynamic admissibility of light efficiencies larger than unity," Sov. Phys. JETP **41**, 613–616 (1976).
31. P. T. Landsberg and D. A. Evans, "Thermodynamic limits for some light-producing devices," Phys. Rev. **166**, 242–246 (1968).